JOURNAL OF GEOPHYSICAL RESEARCH: OCEANS, VOL. 118, 1–10, doi:10.1002/jgrc.20253, 2013

Longitudinal variability of size-fractionated N_2 fixation and DON release rates along 24.5°N in the subtropical North Atlantic

Mar Benavides,[1] Deborah A. Bronk,[2] Nona S. R. Agawin,[3] M. Dolores Pérez-Hernández,[1] Alonso Hernández-Guerra,[1] and Javier Arístegui[1]

Received 18 April 2013; accepted 21 May 2013.

[1] Dinitrogen (N_2) fixation and dissolved organic nitrogen (DON) release rates were measured on fractionated samples (>10 μm and <10 μm) along 24.5°N in the subtropical North Atlantic. Net N_2 fixation rates (N_2 assimilation into biomass) ranged from 0.01 to 0.4 nmol N L^{-1} h^{-1}, and DON release rates ranged from 0.001 to 0.09 nmol N L^{-1} h^{-1}. DON release represented ~14% and ~23% of >10 μm and <10 μm gross N_2 fixation (assimilation into biomass plus DON release), respectively. This implies that by overlooking DON release, N_2 fixation rates are underestimated. Net N_2 fixation rates were higher in the east and decreased significantly toward the west ($r_s = -0.487$, $p = 0.002$, and $r_s = -0.496$, $p = 0.001$, for the >10 μm and <10 μm fractions, respectively). The sum of both fractions correlated with aerosol optical depth at 550 nm (AOD 550 nm) ($r_s = 0.382$, $p = 0.017$) and phosphate (PO_4^{3-}) concentrations ($r_s = 0.453$, $p = 0.018$), suggesting an enhancement of diazotrophy as a response to aerosol inputs and phosphorus availability. In contrast, DON release was constant among size fractions and did not correlate with any of these variables. We also compared N_2 fixation rates obtained using the $^{15}N_2$ dissolved and bubble methods. The first gave average rates 50% (49% ± 39) higher than the latter, which supports the finding that previously published N_2 fixation rates are likely underestimated. We suggest that by combining N_2 fixation and DON release measurements using dissolved $^{15}N_2$, global N_2 fixation rates could increase enough to balance oceanic fixed nitrogen budget disequilibria.

Citation: Benavides, M., D. A. Bronk, N. S. R. Agawin, M. D. Pérez-Hernández, A. Hernández-Guerra, and J. Arístegui (2013), Longitudinal variability of size-fractionated N_2 fixation and DON release rates along 24.5°N in the subtropical North Atlantic, *J. Geophys. Res. Oceans*, *118*, doi:10.1002/jgrc.20253.

1. Introduction

[2] Most of the nitrogen (N) needed for primary production reaches the euphotic zone through upwelling and diffusion of cold nutrient-rich waters from the deep sea. However, in the subtropical gyres of the oceans, the entrance of nutrients from the deep to the upper layer is hindered by the strong water column stratification maintained almost continuously throughout the year by solar heating of the ocean surface and the circulation patterns derived from trade winds [*Falkowski*, 1997]. In these oligotrophic systems, dinitrogen (N_2) fixation—the reduction of N_2 to ammonium (NH_4^+) by diazotrophic organisms—is important because it provides a new source of N to these stratified N-limited systems [*Mahaffey et al*., 2005].

[3] Besides its importance in fueling primary production, there is a high interest in obtaining an accurate estimate of the global N_2 fixation rate that can balance fixed N losses through denitrification and anammox, presently estimated at ~200 Tg N y^{-1} [*Mahaffey et al*., 2005; *Codispoti*, 2007]. A recent revision of the $^{15}N_2$ tracer method used to measure N_2 fixation indicates that previously measured rates could be underestimated to a great extent [*Mohr et al*., 2010]. This finding raises the question whether a wide application of the revised method in the global oceans would reconcile gains and losses, balancing the oceanic N budget [*Großkpof et al*., 2012; *Wilson et al*., 2012].

[4] Another potentially important source of underestimation in measured N_2 fixation rates is the release of recently fixed N_2. *Glibert and Bronk* [1994] reported that the filamentous nonheterocystous diazotrophic cyanobacterium *Trichodesmium* released ~50% of its recently fixed N_2 in the form of dissolved organic nitrogen (DON) and *Capone et al*. [1994] found evidence that the DON released was largely in the form of amino acids. The DON release

[1]Instituto de Oceanografía y Cambio Global, Universidad de Las Palmas de Gran Canaria, Las Palmas de Gran Canaria, Las Palmas, Spain.
[2]Department of Physical Sciences, College of William and Mary, Virginia Institute of Marine Science, Gloucester Point, Virginia, USA.
[3]Departament de Biologia, Universitat de les Illes Balears, Palma de Mallorca, Spain.

Corresponding author: M. Benavides, Instituto de Oceanografía y Cambio Global, Universidad de Las Palmas de Gran Canaria, Las Palmas de Gran Canaria, ES-35017 Las Palmas, Spain.
(mar.benavides101@doctorandos.ulpgc.es)

2169-9275/13/10.1002/jgrc.20253

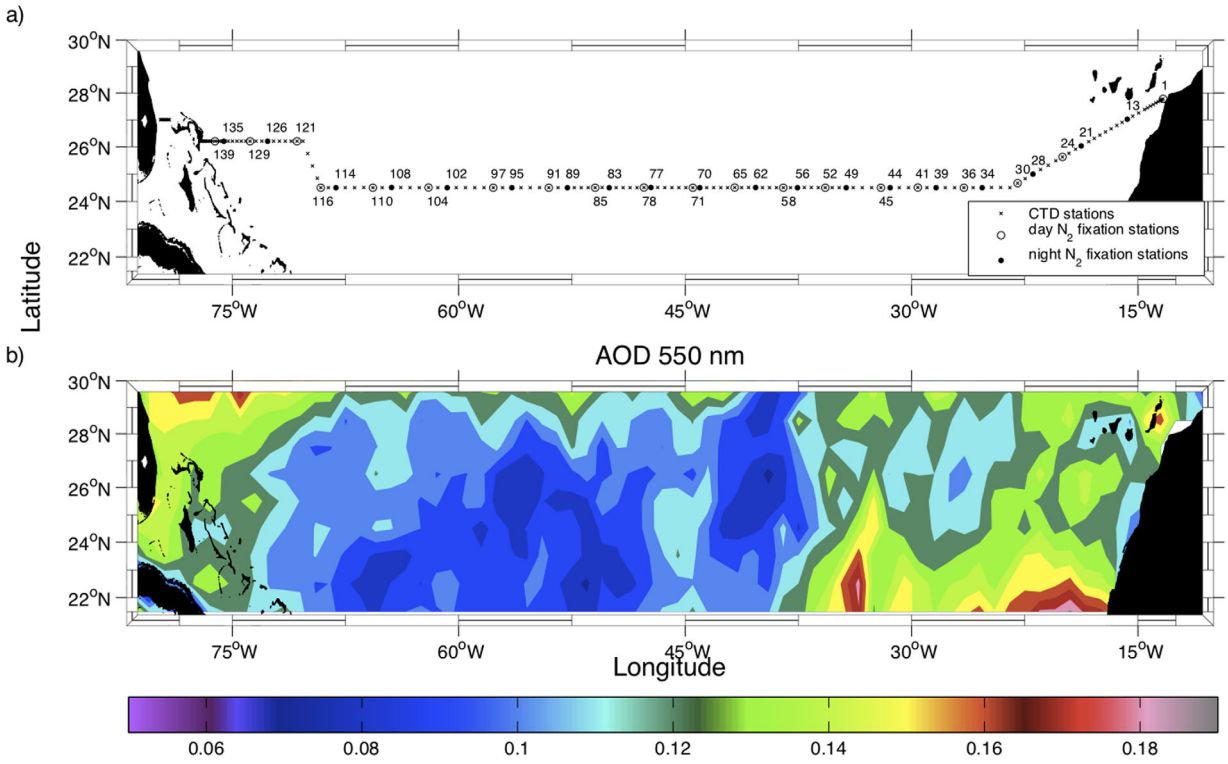

Figure 1. (a) Map of stations sampled along the transect. CTD stations are represented as crosses. Stations were N_2 fixation experiments were performed during the day and during the night are represented as closed and open circles, respectively. (b) Aerosol optical depth (AOD) at 550 nm averaged from 28 January to 9 March 2011. The image was downloaded from the National Aeronautics and Space Administration (NASA) Goddard Earth Sciences Data and Information Services Center Giovanni (NASA GES DISC) online database.

activity of widespread unicellular diazotrophic cyanobacteria (UCYN) has not been studied directly however [*Mulholland*, 2007]. This DON flux is generally unaccounted for in N_2 fixation studies, leading to potential underestimations of total N_2 fixation rates.

[5] Finally, global N_2 fixation rates can be miscalculated when regional estimates are extrapolated to larger oceanic basins or the global ocean. The North Atlantic Ocean is the basin where the greatest quantity of N_2 fixation and diazotrophic diversity data are available, and therefore N_2 fixation rates obtained here have been frequently used to calculate global oceanic rates. As we move forward in the investigation of oceanic N disequilibrium, more detailed spatial and temporal variability of diazotroph assemblages and their diazotrophic activity are needed.

[6] With the aim of covering the longitudinal variability of N_2 fixation rates in the subtropical North Atlantic and to avoid underestimations, we measured fractionated N_2 fixation and DON release rates at 40 stations over the 24.5°N parallel using the improved $^{15}N_2$ tracer technique [*Glibert and Bronk*, 1994; *Mohr et al*., 2010].

2. Materials and Methods

2.1. Hydrographic Measurements and Nutrients

[7] Sampling was performed crossing the North Atlantic Ocean from the northwest (NW) African coast (Cape Jubi) to the Bahamas onboard the R/V *Sarmiento de Gamboa* from 27 January to 15 March 2011. The major part of the cruise was conducted over 24° 30′ N (World ocean circulation experiment—WOCE—section A05) (Figure 1a). Temperature, salinity, and fluorescence data were recorded with a SeaBird 911 plus conductivity, temperature and depth probe (CTD) equipped with redundant temperature and salinity sensors and a Sea-Tech fluorometer, all mounted on a General Oceanics 24 Niskin bottle rosette sampler. At each station, temperature and salinity were measured from the surface down to 20 m above the seafloor. Water samples were collected at each station in order to calibrate salinity values using a Guildline AUTOSAL model 8400B salinometer with a precision better than 0.002 for single samples.

[8] Samples for nutrient analyses were collected from the rosette Niskin bottles in 15 mL polypropylene tubes and immediately frozen until analysis ashore. The concentrations of nitrate (NO_3^-), nitrite (NO_2^-), NH_4^+, phosphate (PO_4^{3-}), and silicon (SiO_2) were determined with a Technicon segmented-flow autoanalyzer. Standard methods were modified to obtain a detection limit of 2 nmol L^{-1} [*Raimbault et al*., 1990; *Kérouel and Aminot*, 1997].

2.2. Sea Surface Height Anomalies and Atmospheric Dust

[9] Daily sea level anomaly (sea surface height anomaly (SSHA)) data (the difference between the total SSH and the average SSH for this time of year) were downloaded from the archiving, validation, and interpretation of

satellite oceanographic remote sensing service (AVISO, http://www.aviso.oceanobs.com/). The daily data were averaged for each three N_2 fixation stations.

[10] Aqua-MODIS aerosol optical depth at 550 nm (AOD 550 nm) can be used as a proxy for dust presence in the atmosphere [*Kaufman et al*., 2005]. In order to assess the effect of atmospheric dust on N_2 fixation rates, we used AOD 550 nm data obtained from the National Aeronautics and Space Administration (NASA) Goddard Earth Sciences Data and Information Services Center Giovanni (NASA GES DISC) online database. The spatial distribution of AOD 550 nm during our cruise is plotted in Figure 1b.

2.3. Fractionated Net N_2 Fixation and DON Release Rates

[11] Rates of N_2 fixation and DON release were measured in the >10 μm and <10 μm size fraction of samples collected from the surface (~5 m). The size fractionation was done at the start of the incubation. We sampled one station per day but alternated between day (0900–1200) and night samplings (1900–2100, local time) (Figure 1a). This approach allowed us to study the diazotrophic activity of organisms that fix N_2 in the light (e.g., *Trichodesmium*), and organisms that only fix N_2 in the dark to avoid oxygen deactivation of the nitrogenase enzyme system (e.g., *Crocosphaera*).

[12] N_2 fixation and DON release rates were measured using ^{15}N-labeled N_2 gas during 3–4 h incubations. There are two general approaches used to add the labeled gas to a sample: the addition of water that was saturated with $^{15}N_2$ [e.g., *Glibert and Bronk*, 1994; *Mohr et al*., 2010], and the addition of a bubble [*Montoya et al*., 1996]. In this study, we used the addition of saturated water in fractionated seawater samples and the bubble method in whole (unfiltered) seawater samples (see below). With the addition of a bubble, the N_2 fixation rate is potentially underestimated due to slow dissolution of the gas bubble in water [*Mohr et al*., 2010].

[13] To prepare the $^{15}N_2$-saturated water, surface seawater (~5 m) was recovered from the flow-through system of the ship and filtered through a 47 mm GF/F filter. This was done during the upcast of the CTD to ensure that the $^{15}N_2$-saturated water was the same as the sample water. This filtered seawater was decanted into 0.5 L transparent polycarbonate bottles (Nalgene) and degassed as outlined in *Mohr et al*. [2010]. Each bottle was filled to overflow, closed with a septum screw-cap and 5 mL of $^{15}N_2$ (99 at % ^{15}N; Cambridge Isotope Laboratories) were injected using a Hamilton gas-tight syringe. The bottles were vigorously shaken for 10–20 min until the bubble was fully dissolved and then kept in the on-deck incubators until the rosette was back on board (0.5–2.5 h depending on the station depth) to ensure that the ^{15}N-enriched seawater had the same temperature as the sample at the time of mixing, in order to protect the organisms from thermal shocks.

[14] To check the real ^{15}N enrichment of the $^{15}N_2$-amended seawater added to the samples, replicate samples of the $^{15}N_2$-amended seawater prepared on board were taken in 10 mL crimp vials (Chrompack), filled to overflow, and sealed with teflon-lined stoppers and aluminum caps using a seal crimper. These were stored at room temperature in the dark until being analyzed by membrane inlet mass spectrometry (MIMS) in S. Joye's lab. MIMS analysis showed that the real enrichment of the $^{15}N_2$-amended seawater was ~100% ($99 \pm 2\%$) of that expected from complete dissolution of the $^{15}N_2$ bubble.

[15] To collect water used to measure fractionated rates, near surface (~5 m) seawater was collected with a 30 L Niskin bottle at each station. The samples were prefractionated by filtering two 2 L replicates through a 10 μm Nitex custom-made sieve. The <10 μm fraction was recovered in 2.4 L transparent polycarbonate bottles (Nalgene). The >10 μm fraction was recovered from the sieve by gently washing and concentrating the biological material using a water sprayer filled with filtered (GF/F) seawater from the same station. Then, 200 mL of $^{15}N_2$-enriched filtered seawater was added to all bottles, they were filled to the top with filtered seawater and placed in the on-deck incubators for 3–4 h. The incubators were connected to the ship's flow-through system and covered with neutral density screens (Lee Filters). After the incubation, the samples were filtered through precombusted 25 mm GF/F filters, which were subsequently stored in sterile cryovials (VWR) and frozen. The GF/F filtrates were then filtered through 0.2 μm polycarbonate filters (GE-Osmonics Poretics) using gentle vacuum pressure (<100 mm Hg) to remove bacteria prior to isolating the dissolved N pools. Rigorous care was taken to avoid light stress in the samples. The filtrates were stored frozen in triplicate 50 mL polypropylene tubes (VWR) and used to measure the concentrations of NO_3^-, NO_2^-, NH_4^+, and total dissolved N (TDN), and the ^{15}N atom % enrichment of NO_3^-, NH_4^+, and TDN as described in section 2.5.

2.4. Whole Seawater Net N_2 Fixation Rates

[16] Parallel to seawater collection for fractionation, whole surface seawater was transferred from the 30 L Niskin bottle to 2.4 L transparent polycarbonate bottles. The bottles were completely filled using silicone tubing to prevent the introduction of air bubbles. They were then sealed with septum screw caps before 2 mL of ^{15}N-labeled N_2 gas were injected through the septum. The pressure across the septum was equilibrated by allowing the excess water to escape through a sterile syringe tip piercing the septum. The bottles were placed in the on-deck incubator for the same incubation period. After the incubation, samples were also filtered through precombusted GF/F filters, stored in cryovials, and frozen until isotope ratio mass spectrometer (IRMS) analysis ashore. N_2 fixation rates measured with the bubble method were calculated as outlined in *Montoya et al*. [1996].

2.5. Chemical Analyses and Rate Calculations

[17] Nutrient pools in filtrates (surface seawater samples incubated with $^{15}N_2$ and filtered through GF/F and 0.2 μm, see above) were analyzed in D. Bronk's lab after the cruise. Concentrations of NH_4^+ were analyzed in duplicate with the manual phenol hypochlorite method [*Hansen and Koroleff*, 1983] using a Shimadzu UV-1601 spectrophotometer (detection limit of ~0.03 μmol L^{-1}). Concentrations of NO_3^- and NO_2^- were determined with a Lachat QuikChem 8500 autoanalyzer (detection limits of 0.1 and 0.03 μmol L^{-1}, respectively). TDN concentrations were analyzed on a Shimadzu TOC-V equipped with a total nitrogen module (TNM). DON concentrations were calculated by subtracting NO_3^-, NO_2^-, and NH_4^+ concentrations from TDN concentrations; propagation of error calculations were used to estimate errors associated with DON concentrations [*Bronk et al*., 2000].

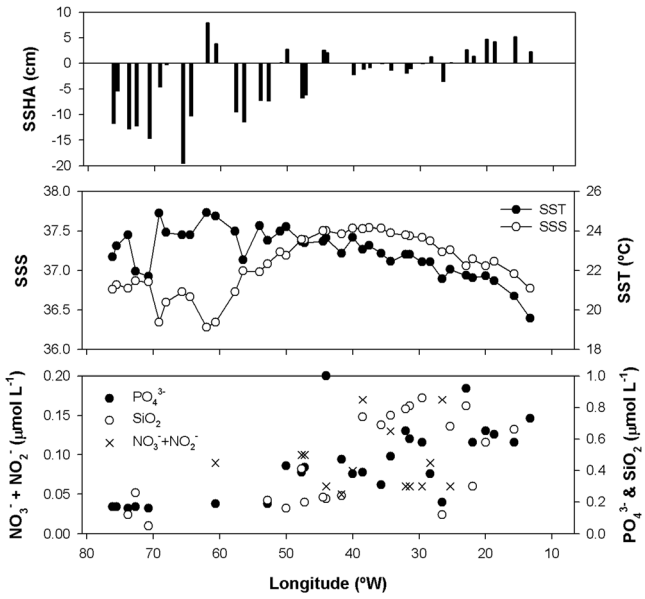

Figure 2. Values of (a) sea surface height anomalies (SSHA), (b) sea surface temperature (SST) and sea surface salinity (SSS), and (c) surface concentrations of nitrate plus nitrite ($NO_3^- + NO_2^-$), phosphate (PO_4^{3-}) and silicon (SiO_2) at stations were N_2 fixation experiments were performed.

[18] The ^{15}N atom % enrichment of the NO_3^-, NH_4^+, and TDN pools was determined to allow the quantification of DON release rates. To isolate the NH_4^+ pool, we used solid phase extraction (SPE) columns (C_{18}) [*Dudek et al*., 1986] and then spotted the isolated NH_4^+ onto a precombusted GF/F filter using a pipette prior to mass spectrometry analysis. The ^{15}N atom % enrichment of the particulate organic N (PON) and NH_4^+ pools were analyzed on a Europa GEO 20/20 IRMS with an automated N and carbon analyzer for solids and liquids (ANCA-SL). To isolate the TDN pool, 15 mL subsamples of the filtrate were oxidized to NO_3^- via persulfate oxidation [*Valderrama*, 1981]. The NO_3^- was then converted to nitrous oxide (N_2O) using denitrifying bacteria lacking N_2O-reductase activity [*Sigman et al*., 2001]. Isotope ratios of N_2O were then measured using a ThermoFinnigan GasBench + PreCon trace gas concentration system interfaced to a ThermoScientific Delta V Plus IRMS at the University of California Davis Stable Isotope Facility (Davis, CA). The same approach without the persulfate oxidation step was used to isolate the NO_3^- pool. The atom % enrichment of TDN and NO_3^- was analyzed in single samples (one replicate was used for each of the two analyses) and that is why standard deviation error bars are not available in Figure 5.

[19] The ^{15}N atom % enrichment of each of these pools was used to measure DON release rates as follows:

$$\begin{aligned}(\text{atom \% TDN} \times [\text{TDN}]) = {} & \left(\text{atom \%NO}_3^- \times \left[\text{NO}_3^-\right]\right) \\ & + \left(\text{atom \%NH}_4^+ \times [\text{NH}_4^+]\right) \\ & + (\text{atom \%DON} \times [\text{DON}]) \end{aligned} \quad (1)$$

where [TDN], [NO_3^-], [NH_4^+], and [DON] are the concentrations of TDN, NO_3^-, NH_4^+, and DON, respectively.

[20] Solving equation (1), the ^{15}N atom % enrichment of the DON pool was calculated as follows:

$$\text{Atom \% DON} = \frac{(\text{atom \%TDN} \times [\text{TDN}]) - \left(\left(\text{atom \%NO}_3^- \times \left[\text{NO}_3^-\right]\right) + \left(\text{atom \%NH}_4^+ \times \left[\text{NH}_4^+\right]\right)\right)}{[\text{DON}]} \quad (2)$$

[21] N_2 fixation and DON release rates were then calculated using standard tracer equations:

$$\text{Rate} = \left(\frac{\text{atom \%excess target pool}}{\text{atom \%excess source pool} \times \text{time}}\right) \times \text{target pool concentration} \quad (3)$$

where atom% excess is the ^{15}N% enrichment over natural abundance.

[22] N_2 fixation rates obtained from $^{15}N_2$ incorporation into biomass were considered "net" N_2 fixation rates. The sum of net N_2 fixation rates and DON release rates were considered "gross" N_2 fixation rates [*Mulholland et al*., 2004].

3. Results

3.1. Hydrographic Features and Nutrient Concentrations

[23] Low values of sea surface temperature (SST) and sea surface salinity (SSS) of ~19°C and 36.8, respectively, were observed near the coastal upwelling off NW Africa (Figure 2). From east to west, SST increased up to 24.26°C at 54.03°W, and SSS up to 37.54 at 37.57°W. Moving westward, SST presented sharp decreases of 1–2°C coincident with strong negative SSHA (<−12 cm). In contrast, SSS decreased until 62°W (station 104), where it reached 36.28. From 62°W to the west, SSS increased in two steps coincident with positive or low values of SSHA, and finally reached ~36.74.

[24] The surface concentrations of $NO_3^- + NO_2^-$, PO_4^{3-}, and SiO_2 were generally maximum at the eastern end of the transect (coinciding with the NW African coastal upwelling), and decreased toward the west. The lowest concentrations were observed west of ~45°W, coinciding with the oligotrophic Sargasso Sea.

[25] Along with SST and SSS increments and high values for nutrients, the first seven N_2 fixation stations showed positive SSHA values, which then decreased considerably until station 71 (44.5°W). From this position to the west, high and predominantly negative SSHA dominated.

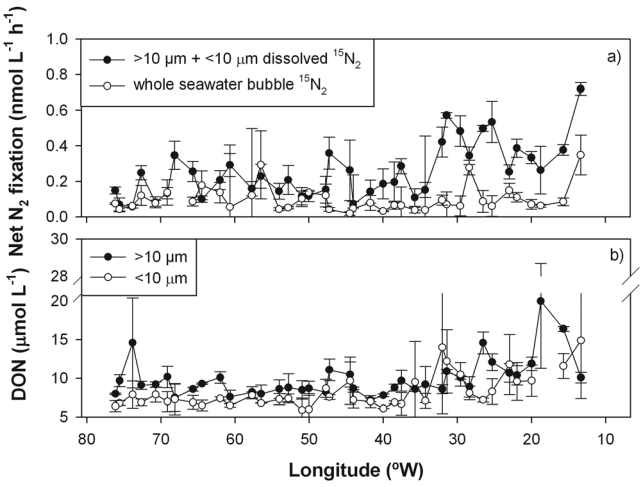

Figure 3. (a) N_2 fixation rates obtained as the sum of >10 µm and <10 µm rates using the $^{15}N_2$ dissolved method ($n = 39$), and by incubation of whole seawater with a $^{15}N_2$ bubble ($n = 38$). (b) DON concentrations (in µ*M*) in the filtrates of the incubation bottles containing the >10 µm and <10 µm planktonic fractions after 3–4 h incubation with $^{15}N_2$ ($n = 76$ per each fraction). Error bars represent the standard deviation of the mean.

3.2. Dissolved $^{15}N_2$ Versus $^{15}N_2$ Bubble Net N_2 Fixation Rates

[26] The sum of net N_2 fixation rates in the >10 µm and <10 µm fractions measured using the dissolved method [*Mohr et al*., 2010] was compared to net N_2 fixation rates (in whole seawater samples collected at the same stations) using the $^{15}N_2$ bubble method [*Montoya et al*., 1996]. The difference between both rates tended to increase toward the east (Figure 3a). Indeed, the percent underestimation of the bubble method (average 49 ± 39%; range 6–93%) was significantly correlated with longitude ($r_s = 0.518$, $p = 0.001$). The concentrations of DON in >10 µm and <10 µm samples did not correlate significantly with the percentage underestimation of N_2 fixation rates, but followed a similar longitudinal distribution (Figure 3b).

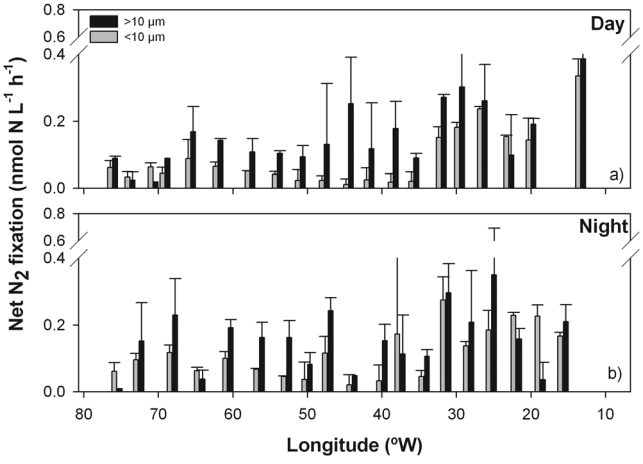

Figure 4. (a) The >10 µm and <10 µm net N_2 fixation rates in stations sampled during the day, and (b) during the night (>10 µm $n = 76$, <10 µm $n = 78$). Error bars represent the standard deviation of the mean.

3.3. N_2 Fixation and DON Release Estimated by the Dissolved $^{15}N_2$ Method

[27] Both >10 and <10 µm organisms presented a similar range of N_2 fixation rates (~0.01 to ~0.44 nmol N L^{-1} h^{-1}), although >10 µm rates were statistically different from <10 µm rates (Wilcoxon test, $p < 0.0001$). On average, net N_2 fixation rates of organisms >10 µm were slightly higher than those <10 µm (0.16 and 0.1 nmol N L^{-1} h^{-1}, respectively). Both rates showed a tendency to decrease toward the west (Figure 4), showing significant relationships with longitude (Spearman's correlation rank coefficient $r_s = -0.487$, $p = 0.002$, and $r_s = -0.496$, $p = 0.001$, for the >10 µm and <10 µm fractions, respectively). N_2 fixation rates of organisms >10 µm measured during the day were not significantly different from those measured during the night (Wilcoxon test, $p = 0.936$), while the differences between rates of organisms <10 µm measured during the day and the night were almost statistically significant (Wilcoxon test, $p = 0.059$). In most stations, N_2 fixation rates measured during the night were higher than those measured during the day for both >10 µm and <10 µm fractions (Figure 4).

[28] DON release rates in organisms >10 µm and <10 µm ranged from 0.001 to ~0.09 nmol N L^{-1} h^{-1} (Figure 5). Considering gross N_2 fixation as net N_2 fixation plus DON release [*Mulholland et al*., 2004] DON release represented ~14% of >10 µm gross N_2 fixation and ~23% of <10 µm gross N_2 fixation (data not shown). Significant differences in DON release were not found between >10 µm and <10 µm fractions, neither between day and night (Wilcoxon test, $p > 0.05$). Also, DON release rates did not show a clear trend with longitude ($r_s = 0.203$, $p = 0.391$, and $r_s = -0.046$, $p = 0.848$, for the >10 µm and <10 µm fractions, respectively).

4. Discussion

4.1. Dissolved Versus Bubble Methods

[29] Using the dissolved $^{15}N_2$ method, in this study we have measured N_2 fixation rates on average 50% higher than those estimated using the $^{15}N_2$ bubble method. This difference between the two methods is at the lower end of the few comparisons available in the literature. *Mohr et al*. [2010] observed that N_2 fixation rates in cultures of

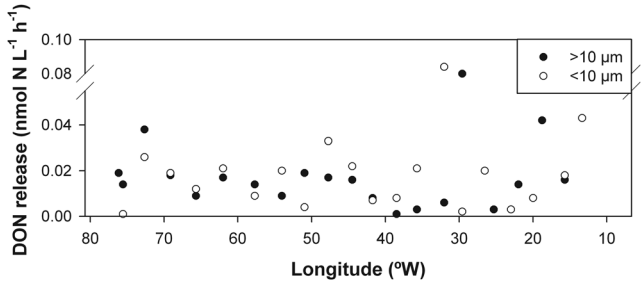

Figure 5. DON release rates in the >10 µm and <10 µm size fractions.

Crocosphaera watsonii were 40% higher when the dissolved method was used, compared to the bubble method. Recently, *Wilson et al*. [2012] compared both methods in natural waters of the North Pacific Ocean (station ALOHA), and obtained rates that were 2–3.5 fold higher with the dissolved method than they were with the bubble method. *Großkopf et al*. [2012] observed that both methods differ by 62% when the diazotrophic community is dominated by *Trichodesmium*, and up to 570% when dominated by diazotrophs other than *Trichodesmium* (symbionts of diatoms, UCYN, heterotrophic diazotrophs). Adding to differences in the diazotrophic community, the factors influencing N_2 fixation differences between the dissolved and bubble methods include (1) temperature, which affects gas dissolution into water, (2) the agitation of the incubation bottles, (3) the volume of the incubation bottle, (4) the volume of $^{15}N_2$ injected, (5) the duration of the incubation, (6) the time the incubation starts relative to the onset of nitrogenase activity, which differs among diazotroph species, and (7) the DOM coating of the $^{15}N_2$ bubble [*Mohr et al*., 2010]. These factors vary widely among the previously published N_2 fixation data measured using the bubble method, which makes the recalculation of rates difficult if not impossible [*Großkopf et al*., 2012].

[30] This study does not include diazotrophic organisms' abundance and distribution data, so we cannot analyze how this affected the percentage underestimation of the bubble method with regards to the dissolved method. However, a recent compilation of diazotroph abundance data [*Luo et al*., 2012] shows that *Trichodesmium* clearly dominates in the tropical Northwest Atlantic, while UCYN are somewhat more abundant in the eastern than in the western side of the basin and at higher latitudes. This distribution of diazotrophs and percentage underestimation by the bubble method versus the dissolved method agrees with *Großkopf et al*. [2012], although our percentage underestimation values are much lower. During our cruise, *Mompeán et al*. [2013] measured the abundance of *Trichodesmium* using vertical net tows. These authors observed that *Trichodesmium* was almost absent from the beginning of the transect (NW African coast) until ~25°W, followed by a peak of ~15 trichomes L^{-1} at ~30°W, and decreased toward the west. This longitudinal distribution is contrary to the arguments of *Großkopf et al*. [2012]. However, the low abundance of *Trichodesmium* recorded suggests that their role in the diazotrophic activity measured in our experiments was minor.

[31] With regards to the potential effect of DOM in slowing the dissolution of the $^{15}N_2$ bubble, we checked for any significant correlations between percentage underestimations and DON concentrations. Correlations between DON and the difference between the dissolved and bubble methods were not statistically significant (data not shown), but their longitudinal trend was similar. We observed that the differences between the dissolved and bubble methods were greater in the eastern part of the transect, coinciding with higher DON concentrations (Figure 3b). The difference between both methods would have probably correlated better with dissolved organic carbon (DOC) since it is a better proxy for the total DOM pool. Oceanic DOC concentrations range from 34 to >90 μ*M*, while DON concentrations range from 2 to 13 μ*M* [*Hansell and Carlson*, 2002]. Unfortunately, DOC data are not available in this case.

[32] Another factor specific to this study that may have influenced differences between both methods is the prefractionation of samples prior to incubation with $^{15}N_2$. The sum of fractionated N_2 fixation rates (>10 μm + <10 μm) may be not directly comparable to whole seawater N_2 fixation rates, and sample fractionation is not always successful. For example, <10 μm organisms may be retained in the >10 μm fraction due to clogging of the mesh used for fractionation. However, due to the oligotrophic character of the area of study, seawater samples flowed easily through the mesh used for fractionation, and thus significant clogging or cell disruption may have not been significant.

[33] Finally, we must consider that the short incubation period used in our study (3–4 h) diminishes the dissolution of the $^{15}N_2$ bubble in the seawater sample in comparison with 24 h incubations conducted in other studies, which together with the large standard deviation found between methods (% underestimation = 49 ± 39%; see section 3) suggests that the underestimation of rates when using the $^{15}N_2$ bubble method could have been less severe if a longer incubation period had been chosen. As an alternative to the preparation of $^{15}N_2$-enriched seawater to conduct N_2 fixation assays and to avoid any uncertainties related to this new method until it is definitely widely proven and a general protocol is established, we recommend to monitor the equilibration of the $^{15}N_2$ bubble during the incubation period in order to calculate accurate N_2 fixation rates.

4.2. DON Release

[34] DON release rates were not significantly different between fractions, nor were they different between day and night, or significantly correlated with longitude. This lack of spatial and daily variability in both size fractions suggests that the release of a percentage of recently fixed N_2 is inherent to natural assemblages of marine diazotrophs, although we cannot discern if this release was active or passive, via predation, viral infection, or cell death.

[35] We must note that the DON release rates presented here may be biased by the methodological approach used. The fractionation of seawater samples into >10 μm and <10 μm fractions prior to incubation with $^{15}N_2$ could have disrupted cells, artificially inflating DON release rates. However, the differences between prefractionation and postfractionation NH_4^+ concentration—an indicator of cell breakage [*Bronk and Glibert*, 1993]—were not significant for either fraction (*t*-test, $p = 0.92$ and $p = 0.13$ for the >10 μm and <10 μm fractions, respectively, data not shown), suggesting that the DON release rates presented here are robust. Another factor potentially influencing the DON release rates presented here is the disruption of trophic interactions between different sized microorganisms occasioned when incubated separately [*Havens*, 2001]. If the separate incubation of >10 μm and <10 μm diazotrophs had any effect on their DON release rates, we could not quantify it. Prefractionation has been previously used in a number of studies [e.g., *Bronk and Glibert*, 1993; *Ohlendieck et al*., 2000; *Benavides et al*., 2011] and has been used here because it is the only possible approach to measure fractionated DON release rates.

Table 1. Fractionated Net N_2 Fixation Rates, DON Release Rates, and the Percent Contribution of DON Release to Gross N_2 Fixation[a]

	Net N_2 Fixation		DON Release		% DON Release	
Zone	>10 μm	<10 μm	>10 μm	<10 μm	>10 μm	<10 μm
+SSHA	0.19 ± 0.10	0.14 ± 0.10	0.02 ± 0.02	0.02 ± 0.03	10.89 ± 16.08	22.15 ± 21.63
−SSHA	0.12 ± 0.07	0.06 ± 0.03	0.02 ± 0.01	0.02 ± 0.01	17.95 ± 15.90	23.42 ± 16.34

[a]Rates are in nmol L^{-1} h^{-1}. Values represent the average and standard deviation (average ± SD). The +SSHA zone comprises stations 1–71, or longitude 13.34–44.5° W. The −SSHA zone comprises stations 77–139, longitude 44.5–76.15° W).

[36] Previous studies of diazotrophic DON release have focused on the filamentous cyanobacterium *Trichodesmium* [*Glibert and Bronk*, 1994]. These authors found that *Trichodesmium* released 50% of their recently fixed N_2 as DON, implying that true N_2 fixation rates were considerably underestimated if DON release was not taken into account. The release of DON by other diazotrophs has not been studied directly in the field and therefore it is difficult to put the results obtained here into context. However, when our hourly surface DON release rates are integrated to 100 m and scaled up to days, the average integrated DON release rates obtained (up to 0.75 μmol N m^{-2} d^{-1}) are in the range of the N_2 fixation in the <0.7 μm fraction (seawater filtered through a GF/F) obtained by *Konno et al*. [2010]. Nonetheless, we must note that the DON release rates measured here result from the quantification of the ^{15}N atom% enrichment of the DON pool (in filtrates of samples passed through GF/F filters and 0.2 μm PC filters) and not of any particles (organic or inorganic) <0.7 μm. In another attempt to measure DON release rates using axenic cultures of *Cyanothece* sp. Miami BG 043511 grown in optimum conditions, we found that this organism releases only ∼1% of their recently fixed N_2 as DON [*Benavides et al*., 2013]. This is much lower than the ∼23% DON release obtained in this study for the <10 μm fraction. However, *Cyanothece* or other closely related UCYN belonging to group C (UCYN-C) diazotrophs are less frequent in the North Atlantic Ocean, and therefore it can be expected that the <10 μm diazotroph community in this transect was more likely composed of *Crocosphaera* (UCYN group B—UCYN-B), UCYN of group A (UCYN-A), and heterotrophic diazotrophs [*Langlois et al*., 2008]. The DON release activity of those diazotrophs is unknown [*Mulholland*, 2007], but some evidence is accumulating. The difference between gross N_2 fixation rates obtained using the acetylene reduction assay and net N_2 fixation rates obtained using the $^{15}N_2$ method has been used as a proxy to estimate the release of recently fixed N_2 [*Mulholland et al*., 2004]. *Benavides et al*. [2011] measured both rates on fractionated samples (>10 μm and <10 μm) over the Canary Current and observed that the <10 μm fraction potentially released ∼60% of their recently fixed N_2. In this study, we measured the ^{15}N enrichment of the DON pool and found that both the >10 μm and <10 μm fractions DON release rates represent a significant percentage of gross N_2 fixation. Now that the correction of N_2 fixation rates using the dissolved $^{15}N_2$ method is in the spotlight, we call attention to the inclusion of DON release measurements in routine field samplings. The application of the dissolved method combined with DON release rates could perhaps raise global N_2 fixation rates enough to balance denitrification, balancing the oceanic fixed N budget.

4.3. Longitudinal Variability of N_2 Fixation

[37] In contrast with the general trend of higher N_2 fixation rates in the western Atlantic than in the eastern Atlantic observed in previous studies [*Montoya et al*., 2007; *Luo et al*., 2012], in this study both >10 μm and <10 μm N_2 fixation rates were highest close to the NW African coast and decreased westward (Figure 4). This longitudinal variability could be partly affected by nutrient availability in the upper ocean controlled by diffusion of nutrient-rich deep waters through the thermocline. In the Northern hemisphere, anticyclonic eddies promote positive SSHA, deepening the thermocline and hence enhancing organic matter accumulation and bacterial production within their cores [e.g., *Baltar et al*., 2010]. On the contrary, cyclonic eddies foster negative SSHA, which uplifts the thermocline and promotes the upwelling of deeper nutrient-rich cold waters, enhancing primary production and chlorophyll concentrations [e.g., *Arístegui et al*., 1997]. In contrast to autotrophic phytoplankton species, which depend on NO_3^- upwelled from the deep sea or NH_4^+ regenerated in situ for their growth, diazotrophic organisms are capable of growing on N_2 as the only source of N. Theoretically, this sets out a different scenario for diazotrophs, which would grow better in the core of warm and nutrient-poor anticyclonic eddies, than in that of cold and nutrient-rich cyclonic eddies. *Church et al*. [2009] studied a three-year series of SSHA values at station ALOHA and compared it to N_2 fixation rates and *nifH* gene diversity. These authors observed that pronounced positive SSHA values coincided with enhanced N_2 fixation rates and higher temperatures. However, these authors also pointed out that negative SSHA could promote the upwelling of waters enriched in PO_4^{3-} and SiO_2 relative to fixed N, which would enhance the growth of phosphorus-limited diazotrophs and diatom-diazotroph associations (DDAs) limited by SiO_2. In order to test the hypothesis by *Church et al*. [2009], we operationally divided our transect into two broad areas: an area dominated by weak positive or nearly neutral SSHA values (termed +SSHA zone, east of ∼45° W), and an area where strong negative SSHA values predominate (termed −SSHA zone, west of ∼45° W) (Figure 2a). Similarly to *Church et al*. [2009], N_2 fixation rates were higher where positive SSHA values predominated (+SSHA zone), and lower coinciding with negative SSHA values (−SSHA zone). Indeed, net N_2 fixation rates in >10 μm and <10 μm organisms were significantly different in the two zones (Wilcoxon test, $p = 0.01$ and $p = 0.005$, respectively). Net N_2 fixation rates of the <10 μm fraction were approximately twofold higher in the +SSHA zone than in the −SSHA zone (Table 1),

suggesting that small diazotrophs predominated in the eastern North Atlantic during our sampling. Notwithstanding, the longitudinal tendency of nutrient concentrations observed is opposite to that expected from nutrient diffusion as a consequence of rising or deepening of the thermocline, that is, greater concentrations were observed in the +SSHA zone than in the −SSHA zone (Figure 2c), which covers the oligotrophic Sargasso Sea. Differences in the response of diazotrophic activity to SSHA variability and consequent nutrient inputs to the upper ocean layers between the work of *Church et al*. [2009] and this study might stem from differential atmospheric inputs in the Pacific and Atlantic Oceans. *Voss et al*. [2004] also obtained greater N_2 fixation rates toward the west over 10°N in the north Atlantic. These authors performed their cruise in autumn, when the intertropical convergence zone (ITCZ) reaches its northernmost position enhancing Saharan dust deposition. Our cruise took place in the late winter (January–March 2011), when dust inputs are also known to be maximum [*Torres-Padrón et al*., 2002]. Similar to *Fernández et al*. [2010], we found that total net N_2 fixation rates (>10 μm plus <10 μm) correlated significantly with AOD 550 nm ($r_s = 0.382$, $p = 0.017$), suggesting that nutrients made available through Saharan dust deposition enhance N_2 fixation rates.

[38] Latitudinal gradients in N_2 fixation rates seem to be more abrupt than longitudinal ones. *Moore et al*. [2009] and *Fernández et al*. [2010] observed N_2 fixation rates up to ∼5 and ∼10 nmol L^{-1} d^{-1} (respectively) in the North Atlantic, which decreased to values ∼0 in the South Atlantic. Both authors attributed these latitudinal gradients to differences in dissolved iron availability between the North and South Atlantic basins. Longitudinal gradients in N_2 fixation rates in the North Atlantic are smoother, ranging from ∼0 to 2.5 nmol N L^{-1} d^{-1} [*Voss et al*., 2004; *Montoya et al*., 2007]. Alternative to the role of iron in shaping spatial trends in N_2 fixation rates, *Fernández et al*. [2012] found that under similar dust deposition regimes, the longitudinal variability of N_2 fixation rates may be controlled by phosphorus availability instead. This pattern agrees with the longitudinal trend of PO_4^{3-} concentrations observed here (Figure 2c) and, indeed, PO_4^{3-} concentrations were significantly correlated with total (>10 μm + <10 μm) N_2 fixation rates ($r_s = 0.453$, $p = 0.013$). The agreement between the longitudinal distribution of N_2 fixation rates, AOD 550 nm values and PO_4^{3-} concentrations supports the iron and phosphorus colimitation hypothesis proposed by *Mills et al*. [2004] for the North Atlantic Ocean.

[39] The data compilation of *Luo et al*. [2012] shows that small diazotrophs belonging to UCYN groups A, B, and C are more abundant in the eastern than in the western basin of the North Atlantic and consequently their contribution to total N_2 fixation rates increase to the east, where they dominate over larger diazotrophs such as *Trichodesmium* [*Voss et al*., 2004; *Montoya et al*., 2007; *Benavides et al*., 2011]. Instead, *Trichodesmium* blooms are recurrent in the western North Atlantic where the highest N_2 fixation rates in this basin are found [*Luo et al*., 2012]. In contrast, during this cruise the abundance of *Trichodesmium* was higher in the eastern side of the basin and decreased toward the west [*Mompeán et al*., 2013]. However, the maximum *Trichodesmium* abundances observed are between one and three orders of magnitude lower than observed in previous studies conducted at lower latitudes in the North Atlantic [*Luo et al*., 2012]. The high rates of >10 μm net N_2 fixation observed between the African coast and 20°W during our study (Figure 4a) could not have been supported by the low *Trichodesmium* abundances (∼0) measured by *Mompeán et al*. [2013] in the same longitudinal range, and therefore we infer a low contribution of this genus to the observed N_2 fixation rates in the eastern part of the transect. The contribution of *Trichodesmium* to total N_2 fixation in the rest of the transect (from 20°W to the Bahamas) is uncertain, but given their low abundance we do not believe that this cyanobacterium played an important role in the N_2 fixation rates measured here. In contrast, *Mompeán et al*. [2013] argue that N_2 fixation by *Trichodesmium* largely supported the $\delta^{15}N$ low values observed in different size fractions of the planktonic community during our cruise. However, low $\delta^{15}N$ signals in the planktonic biomass associated to N_2 fixation may be detected in time scales of weeks to months after the N_2 was actually biologically fixed, and thus the results obtained by *Mompeán et al*. [2013] cover a time scale larger than ours (3–4 h incubations). Moreover, the low $\delta^{15}N$ values observed could have been influenced by the deposition of anthropogenic N, a flux which is rapidly approaching the magnitude of oceanic N_2 fixation rates [*Duce et al*., 2008].

[40] Finally, we note that the magnitude of the N_2 fixation rates measured here is difficult to compare with other studies due to the 3–4 h incubation period used (compared to the usual 12–24 h incubations). Moreover, our measurements correspond only to the surface and therefore are not directly comparable to depth-integrated N_2 fixation rates in other studies. The vertical variability of the composition of the diazotrophic community associated with the vertical gradients of light, oxygen, temperature and nutrient availability translates into a vertical variability in N_2 fixation rates. It is generally observed that N_2 fixation rates are highest at the surface and decrease with depth [e.g., *Church et al*., 2009; *Luo et al*., 2012]. Therefore, although the surface N_2 fixation rates presented here are not representative of the whole upper ocean layer, they are still valuable to study the longitudinal variability of diazotrophic activity at a large scale.

5. Conclusions

[41] The results obtained here suggest that the longitudinal variability of N_2 fixation rates in the North Atlantic is affected by atmospheric nutrient inputs and PO_4^{3-} availability, which are maximum in its eastern basin and decrease toward the west. In contrast to net N_2 fixation rates, the release of recently fixed N_2 as DON did not show any longitudinal trend or variability among size fractions. This suggests that this process is inherent of natural assemblages of diazotrophic organisms and should not be overlooked in order to avoid underestimation of true N_2 fixation rates. Moreover, we have added to the body of evidence that N_2 fixation rates are substantially underestimated when the bubble method is used. Measurements of N_2 fixation rates using the dissolved method combined with measurements of DON release in future samplings will probably diminish global N budget unbalances.

[42] **Acknowledgments.** This work was supported by projects Consolider-Malaspina (CSD2008-00077), CAIBEX (CTM2007-66408-CO2-O2), and HOTMIX (CTM2011-30010-C02-01) to J.A., CYFOD (CTM2008-00915-E) to N.S.R.A., and FPI fellowship (BES-2008–006985) to M.B., all from the Spanish Ministry of Science and Innovation (MICINN). We also acknowledge the moderate-resolution imaging spectroradiometer (MODIS) mission scientists, associated National Aeronautics and Space Administration (NASA) personnel and Archiving, Validation, and Interpretation of Satellite Oceanographic Remote Sensing Service (AVISO) scientists for the production of the aerosol optical depth (AOD) and sea surface height (SSH) data used in this study. We greatly thank M. Sanderson, Q. Roberts, L. Killberg Thoreson, R. Sipler, S. Baer, J. Spackeen, and H. Knudsen for their guidance and help with sample and data analysis at VIMS. We also acknowledge J. F. Domínguez-Yanes for providing the nutrient data used in this study, and S. Joye for the MIMS analyses. We are also greatly thankful to the captain and crew of the R/V *Sarmiento de Gamboa* and the UTM for their inestimable help at sea. The sampling methodology used in this study was greatly improved by P. Ferriol.

References

Arístegui, J., et al. (1997), The influence of island-generated eddies on chlorophyll distribution: A study of mesoscale variation around Gran Canaria, *Deep Sea Res. Part I*, *44*(1), 71–96, doi:10.1016/S0967-0637(96)00093-3.

Baltar, F., J. Arístegui, J. M. Gasol, I. Lekunberri, and G. J. Herndl (2010), Mesoscale eddies: Hotspots of prokaryotic activity and differential community structure in the ocean, *ISME J.*, *4*(8), 975–988, doi:10.1038/ismej.2010.33.

Benavides, M., N. S. R. Agawin, J. Arístegui, P. Ferriol, and L. J. Stal (2011), Nitrogen fixation by Trichodesmium and small diazotrophs in the subtropical northeast Atlantic, *Aquat. Microb. Ecol.*, *65*(1), 43–53, doi:10.3354/ame01534.

Benavides, M., N. S. R. Agawin, J. Arístegui, J. Peene, and L. J. Stal (2013), Dissolved organic nitrogen and carbon release by a marine unicellular diazotrophic cyanobacterium, *Aquat. Microb. Ecol.*, *69*(1), 69–80, doi:10.3354/ame01621.

Bronk, D. A., and P. M. Glibert (1993), Contrasting patterns of dissolved organic nitrogen release by two size fractions of estuarine plankton during a period of rapid $NH4^+$ consumption and $NO2^-$ production, *Mar. Ecol. Prog. Ser.*, *96*(3), 291–299.

Bronk, D. A., M. W. Lomas, P. M. Glibert, K. J. Schukert, and M. P. Sanderson (2000), Total dissolved nitrogen analysis: Comparisons between the persulfate, UV and high temperature oxidation methods, *Mar. Chem.*, *69*(1–2), 163–178, doi:10.1016/s0304-4203(99)00103-6.

Capone, D. G., M. D. Ferrier, and E. J. Carpenter (1994), Amino acid cycling in colonies of the planktonic marine cyanobacterium *Trichodesmium thiebautii*, *Appl. Environ. Microbiol.*, *60*(11), 3989–3995.

Church, M. J., C. Mahaffey, R. M. Letelier, R. Lukas, J. P. Zehr, and D. M. Karl (2009), Physical forcing of nitrogen fixation and diazotroph community structure in the North Pacific subtropical gyre, *Global Biogeochem. Cycles*, *23*, GB2020, doi:10.1029/2008GB003418.

Codispoti, L. A. (2007), An oceanic fixed nitrogen sink exceeding 400 Tg N a-1 vs the concept of homeostasis in the fixed-nitrogen inventory, *Biogeosciences*, *4*(2), 233–253, doi:10.5194/bg-4-233-2007.

Duce, R. A., et al. (2008), Impacts of atmospheric anthropogenic nitrogen on the open ocean, *Science*, *320*(5878), 893–897, doi:10.1126/science.1150369.

Dudek, N., M. A. Brzezinski, and P. A. Wheeler (1986), Recovery of ammonium nitrogen by solvent extraction for the determination of relative 15N abundance in regeneration experiments, *Mar. Chem.*, *18*(1), 59–69, doi:10.1016/0304-4203(86)90076-9.

Falkowski, P. G. (1997), Evolution of the nitrogen cycle and its influence on the biological sequestration of CO2 in the ocean, *Nature*, *387*(6630), 272–275.

Fernández, A., B. Mouriño-Carballido, A. Bode, M. Varela, and E. Marañón (2010), Latitudinal distribution of *Trichodesmium* spp. and N_2 fixation in the Atlantic Ocean, *Biogeosciences*, *7*(10), 3167–3176, doi:10.5194/bg-7-3167-2010.

Fernández, A., R. Graña, B. Mouriño-Carballido, A. Bode, M. Varela, J. F. Domínguez-Yanes, J. Escánez, D. de Armas, and E. Marañón (2012), Community N2 fixation and *Trichodesmium spp.* abundance along longitudinal gradients in the eastern subtropical North Atlantic, *ICES J Mar Sci*, doi: 10.1093/icesjms/fss142.

Glibert, P. M., and D. A. Bronk (1994), Release of dissolved organic nitrogen by marine diazotrophic cyanobacteria, Trichodesmium spp, *Appl Environ Microbiol*, *60*(11), 3996–4000.

Großkopf, T., W. Mohr, T. Baustian, H. Schunck, D. Gill, M. M. M. Kuypers, G. Lavik, R. A. Schmitz, D. W. R. Wallace, and J. LaRoche (2012), Doubling of marine dinitrogen-fixation rates based on direct measurements, *Nature*, *488*(7411), 361–364, doi:10.1038/nature11338.

Hansell, D. A., and C. A. Carlson (2002), *Biogeochemistry of Marine Dissolved Organic Matter*, 774 pp., Academic, San Diego, Calif.

Hansen, H. P., and J. Koroleff (1983), *Determination of nutrients, in Methods of Seawater Analysis*, edited by K. Grasshoff, M. Ehrahardt and K. Kremling, pp. 150–157, Wiley-VCH, Weinheim, Germany.

Havens, K. E. (2001), Complex analyses of plankton structure and function, *Sci. World J.*, *1*, 119–132, doi:10.1100/tsw.2001.19.

Kaufman, Y. J., I. Koren, L. A. Remer, D. Tanré, P. Ginoux, and S. Fan (2005), Dust transport and deposition observed from the Terra-Moderate Resolution Imaging Spectroradiometer (MODIS) spacecraft over the Atlantic Ocean, *J. Geophys. Res.*, *110*, D10S12, doi:10.1029/2003jd004436.

Kérouel, R., and A. Aminot (1997), Fluorometric determination of ammonia in sea and estuarine waters by direct segmented flow analysis, *Mar. Chem.*, *57*(3–4), 265–275, doi:10.1016/S0304-4203(97)00040-6.

Konno, U., U. Tsunogai, D. D. Komatsu, S. Daita, F. Nakagawa, A. Tsuda, T. Matsui, Y. J. Eum, and K. Suzuki (2010), Determination of total N_2 fixation rates in the ocean taking into account both the particulate and filtrate fractions, *Biogeosciences*, *7*(8), 2369–2377, doi:10.5194/bg-7-2369-2010.

Langlois, R. J., D. Hummer, and J. LaRoche (2008), Abundances and distributions of the dominant nifH phylotypes in the northern Atlantic Ocean, *Appl. Environ. Microbiol.*, *74*(6), 1922–1931, doi:10.1128/aem.01720-07.

Luo, Y. W., et al. (2012), Database of diazotrophs in global ocean: abundance, biomass and nitrogen fixation rates, *Earth Syst. Sci. Data*, *4*(1), 47–73, doi:10.5194/essd-4-47-2012.

Mahaffey, C., A. F. Michaels, and D. G. Capone (2005), The conundrum of marine N_2 fixation, *Am. J. Sci.*, *305*(6–8), 546–595, doi:10.1038/387272a0.

Mills, M. M., C. Ridame, M. Davey, J. LaRoche, and R. J. Geider (2004), Iron and phosphorus co-limit nitrogen fixation in the eastern tropical North Atlantic, *Nature*, *429*(6989), 292–294, doi:10.1038/nature02550.

Mohr, W., T. Großkopf, D. W. R. Wallace, and J. LaRoche (2010), Methodological underestimation of oceanic nitrogen fixation rates, *PLoS ONE*, *5*(9), e12583, doi:10.1371/journal.pone.0012583.

Mompeán, C., A. Bode, V. M. Benítez-Barrios, J. F. Domínguez-Yanes, J. Escánez, and E. Fraile-Nuez (2013), Spatial patterns of plankton biomass and stable isotopes reflect the influence of the nitrogen-fixer Trichodesmium along the subtropical North Atlantic, *J. Plankton Res.*, *35*(3), 513–525, doi:10.1093/plankt/fbt011.

Montoya, J. P., M. Voss, P. Kähler, and D. Capone (1996), A simple, high-precision, high-sensitivity tracer assay for N_2 fixation, *Appl. Environ. Microbiol.*, *62*(3), 986–993.

Montoya, J. P., M. Voss, and D. Capone (2007), Spatial variation in N_2-fixation rate and diazotroph activity in the Tropical Atlantic, *Biogeosciences*, *4*(3), 369–376, doi:10.5194/bg-4–369-2007.

Moore, M. C., et al. (2009), Large-scale distribution of Atlantic nitrogen fixation controlled by iron availability, *Nat. Geosci.*, *2*(12), 867–871, doi:10.1038/ngeo667.

Mulholland, M. R. (2007), The fate of nitrogen fixed by diazotrophs in the ocean, *Biogeosciences*, *4*(1), 37–51, doi:10.5194/bg-4-37-2007.

Mulholland, M. R., D. A. Bronk, and D. G. Capone (2004), Dinitrogen fixation and release of ammonium and dissolved organic nitrogen by Trichodesmium IMS101, *Aquat. Microb. Ecol.*, *37*(1), 85–94, doi:10.3354/ame037085.

Ohlendieck, U., A. Stuhr, and H. Siegmund (2000), Nitrogen fixation by diazotrophic cyanobacteria in the Baltic Sea and transfer of the newly fixed nitrogen to picoplankton organisms, *J. Mar. Syst.*, *25*(3–4), 213–219, doi:10.1016/s0924–7963(00)00016-6.

Raimbault, P., G. Slawyk, and V. Gentilhomme (1990), Direct measurements of nanomolar nitrate uptake by the marine diatom Phaeodactylum tricornutum (Bohlin). Implications for studies of

oligotrophic ecosystems, *Hydrobiologia*, *207*(1), 311–318, doi:10.1007/bf00041470.

Sigman, D. M., K. L. Casciotti, M. Andreani, C. Barford, M. Galanter, and J. K. Böhlke (2001), A bacterial method for the nitrogen isotopic analysis of nitrate in seawater and freshwater, *Anal. Chem.*, *73*(17), 4145–4153, doi:10.1021/ac010088e.

Torres-Padrón, M. E., M. D. Gelado-Caballero, C. Collado-Sánchez, V. F. Siruela-Matos, P. J. Cardona-Castellano, and J. J. Hernández-Brito (2002), Variability of dust inputs to the CANIGO zone, *Deep Sea Res. Part II*, *49*(17), 3455–3464, doi:10.1016/s0967-0645(02)00091-7.

Valderrama, J. C. (1981), The simultaneous analysis of total nitrogen and total phosphorus in natural waters, *Mar. Chem.*, *10*, 109–122, doi:10.1016/0304–4203(81)90027-X.

Voss, M., P. Croot, K. Lochte, M. Mills, and I. Peeken (2004), Patterns of nitrogen fixation along 10° N in the tropical Atlantic, *Geophys. Res. Lett.*, *31*, L23S09, doi:10.1029/2004gl020127.

Wilson, S. T., D. Böttjer, M. J. Church, and D. M. Karl (2012), Comparative assessment of nitrogen fixation methodologies conducted in the oligotrophic North Pacific Ocean, *Appl. Environ. Microb.*, *78*(18), 6516–6523, doi:10.1128/aem.01146-12.